



Original Research

Electromagnetic induction disinfection applied to cemented knee arthroplasty implants: safety evaluation of potential changes in the bone cement

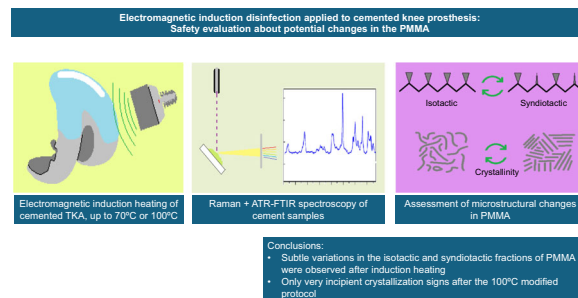
Enrique Cordero García-Galán^{1,6} · Francisco Javier Medel Rezusta² · Héctor Sarnago³ · José M. Burdio³ · Óscar Lucía³ · Jaime Esteban^{4,5} · Enrique Gómez-Barrena⁶

Received: 16 July 2024 / Accepted: 17 February 2025
© The Author(s) 2025

Abstract

Background: Electromagnetic induction heating is a newly developed disinfection method aimed at improving periprosthetic infection outcomes after Debridement and Implant Retention (DAIR). One safety concern is its effect over polymethylmethacrylate (PMMA). The objective of this in-vitro study is to assess such effect on cement adjacent to metallic arthroplasty components. **Methods:** Two different PMMA products, with and without antibiotic, were applied on three total-knee arthroplasty implants. A portable device was used to administer induction-heating protocols: 70 °C, 3.5 min and 100 °C, 3.5 min, while the third prosthesis served as control. The 602 cm⁻¹ and 558 cm⁻¹ bands in Raman spectroscopy were used to assess isotactic and syndiotactic components of PMMA, while 1339 cm⁻¹, 1295 cm⁻¹ and 882 cm⁻¹ bands in infrared spectroscopy (ATR-FTIR) were used to assess crystallinity. **Results:** Isotactic/syndiotactic ratios were 0.27(±0.02) for antibiotic-free cement, and 0.41(±0.02) for gentamicin-loaded cement. After induction-heating protocols, isotactic fraction increased in antibiotic-free cement, and decreased in gentamicin-loaded cement. No evidence of crystallization was found in ATR-FTIR, except for a small increase in 1340 cm⁻¹ band after 100 °C protocol. **Conclusions:** Spectroscopic techniques confirmed that PMMA only experienced minor structural changes after induction heating treatments. From a structural viewpoint, these results suggest that electromagnetic induction heating could be a safe disinfection technique for cemented implants in total knee arthroplasty.

Graphical Abstract



These authors contributed equally: Enrique Cordero García-Galán, Francisco Javier Medel Rezusta

✉ Enrique Cordero García-Galán
enriquecorderogg@gmail.com

- ¹ Dept. of Orthopaedic Surgery and Traumatology, Hospital Universitario Príncipe de Asturias, Av Principal de la Universidad s/n, 28805 Alcalá de Henares, Madrid, Spain
- ² Dept. of Mechanical Engineering. I3A. Escuela de Ingeniería y Arquitectura, Universidad de Zaragoza, Zaragoza, Spain
- ³ Department of Electronic Engineering and Communications. I3A, Universidad de Zaragoza, Zaragoza, Spain

- ⁴ Dept. of Clinical Microbiology, IIS-Fundacion Jimenez Diaz, UAM, Av. Reyes católicos 2, 28040 Madrid, Spain
- ⁵ CIBERINFEC-CIBER de Enfermedades Infecciosas. Av. Monforte de Lemos, 3-5. Pabellón 11. Planta 0, 28029 Madrid, Spain
- ⁶ Present address: Dept of Orthopaedic Surgery and Traumatology. Hospital La Paz-IdiPAZ, Universidad Autónoma de Madrid, Madrid, Spain

1 Introduction

Orthopedic implant infection is a major complication in orthopedic surgery, with an incidence around 2% of all hip and knee arthroplasties [1]. The presence of inert biomaterials adjacent to a joint cavity provides a suitable environment for infecting bacteria to adhere and grow, causing a hindered host's immune response, and the development of bacterial biofilm further reduces antibiotic efficacy as well as phagocytosis. These features make periprosthetic joint infection very difficult to manage. Current therapeutical strategies usually involve multiple surgeries and aggressive antibiotic therapy, often requiring implant removal and prolonged periods of impairment [2–4].

Debridement and Implant Retention (DAIR) is the least aggressive among the current surgical options with curative intention, with limited indications and modest healing rates, currently accepted to be around 50–80% [3]. Some further disinfection methods have been devised in an attempt to enhance healing rates of current treatments. Among those, extrinsic physical agents such as electromagnetic induction heating, electric pulses, photodynamic therapy or high-energy plasma, are in various stages of development [5].

Electromagnetic induction heating takes advantage of the electrical properties of metallic biomaterials to rise the surface temperature of the implant, providing a heat-based surface disinfection technique which is selective to the biomaterial and thus minimizes the thermal effect on host tissues, as well as contactless. Previous in-vitro studies have shown antibacterial efficacy over biofilms of Gram-positive bacteria with temperatures as low as 60 °C for 3.5 min [6]. Other studies by the same group assessed the efficacy of electromagnetic induction heating on planktonic forms, as well as synergistic effects with antibiotics and mechanical scrubbing, and in all cases the bactericidal effect was achieved below 70 °C [7–9].

In order to translate electromagnetic induction heating to clinical practice, one of the main concerns is the effect of temperature protocols on adjacent host tissues, as well as on other biomaterials present in the prosthetic joint. In particular, assessing their effect on surgical cement is key to understanding the applicability of this technique to well-integrated cemented implants.

The main component of surgical cement is polymethylmethacrylate (PMMA), an amorphous thermoplastic polymer. It is often synthesized during implantation surgery from PMMA powder and a solution containing methylmethacrylate monomer and a catalyser. Cement hardening takes place under pressurization between the implant and the underlying bone, in an exothermic reaction which can reach temperatures of 100–110 °C depending on the cement layer width [10, 11]. It is hypothesized that this cement interphase could attenuate thermal diffusion into adjacent

bone, hence working as a protective barrier against thermal bone necrosis. However, to our knowledge, the effect of subjecting already-hardened cement to temperatures greater than 60–70 °C has not been previously studied.

Our research group has developed a portable induction device (Portable Disinfection System based on Induction Heating (PDSIH), Patent solicitude EP22382889.8). This portable design allows for segmental heating of metallic implants with complex geometries and makes it more feasible for its use in the operating room than static induction plates used in previous studies [6–9].

The objective of this in-vitro study is to assess the effect of electromagnetic induction heating protocols on surgical PMMA cement adjacent to metallic arthroplasty components, using the new PDSIH with our current segmental heating protocols.

2 Materials and methods

2.1 Study design

For this in-vitro study, three total knee arthroplasty implants (femoral and tibial metallic components) were cemented with two different PMMA cement products, with and without antibiotic, in the same way PMMA is applied to implants in surgery. The first prosthesis was treated with the standard induction-heating protocol, maintaining 70 °C for 3.5 min (Protocol 1). The second prosthesis was subjected to a modified induction-heating treatment that surpassed 100 °C for 3.5 min, and served as a safety control (Protocol 2). The third prosthesis served as a control, and was left at room temperature at all times (Protocol 3).

Posteriorly, cement samples were retrieved from the fixation surface, and Raman spectroscopy and attenuated total reflectance infrared spectroscopy (ATR-FTIR) were used to assess chemical and microstructural changes in the PMMA polymer.

2.2 Implants and cement

Three units of a posterior-stabilized total knee arthroplasty model frequently used in Orthopedics departments all around the world (Nex Gen®, Zimmer, Warsaw, IN, USA) were selected. Each prosthesis consisted of a Cobalt-Chromium-Molybdenum (CoCrMo) femoral component, and a Titanium-Aluminum-Vanadium (TiAlV) tibial component, apart from other non-metallic components (Polyethylene insert, patellar implant) which were not considered in the present experiment.

Two different PMMA cement products frequently used at our center were selected: radiopaque cement with gentamicin (Simplex® HV with gentamicin Stryker REF



Fig. 1 Gentamicin-bearing cement was applied on the external femoral and tibial compartments, whereas antibiotic-free cement was applied on the internal femoral and tibial compartments

6193-1-001, Stryker Corporation, Kalamazoo, Michigan, USA), and radiopaque cement without antibiotic (Simplex® P Stryker REF 6191-0-001). They were prepared separately in cement mixers at atmospheric pressure. Both were applied on the fixation surface of each component: gentamicin-loaded cement was applied on the lateral femoral and tibial compartments, whereas antibiotic-free cement was applied on the medial femoral and tibial compartments (Fig. 1). Cement was manually pressurized at lab temperature during hardening to obtain a cement layer ranging from 2 to 10 mm.

2.3 Heating protocols

After cement hardening and cooling at lab temperature, electromagnetic induction heating protocols were applied. According to current literature [6, 7, 9, 12], efficacious antibacterial treatments would require surface temperatures of around 70 °C during 3.5 min.

The PDSIH system consisted of an induction coil connected to a DC-AC (direct current to alternate current) power stage, and a DC power supply, all housed inside a sealable insulation housing. The shape of the system, with the induction coil arranged at one end, allowed for segmental treatment of complex. This heating was considerably fast: depending on the geometry and size of the metallic body, target temperatures on the studied components were achieved in a lapse ranging from 30 to 90 s.

No standard protocol for segmental heating of total knee arthroplasty components is currently described in the literature. Thus, the following heating protocols using PDSIH were designed for their feasibility in a surgical environment, with special regard to the limitations of joint exposure in a standard medial parapatellar surgical approach:

To attain 70 °C on the femoral component, PDSIH was manually held 5 mm from the surface, with the potentiometer



Fig. 2 Schematic of standard induction-heating protocol (70 °C, 3.5 min). Fémur (left): slow 10-s sweeping movements are performed 4 times over each trochlear groove alternating direction and side. Two 5-s pulses are applied to each posterior femoral condyle. Tibia (right): a 10-s pulse is applied to the center of the tibial plateau. Two 5-s pulses are applied to each tibial compartment

knob fixed at 100%. Slow 10-s sweeping movements were performed over trochlear grooves alternating direction and side. This process was repeated 4 times for each trochlear groove. Posteriorly, 5-s pulses were applied to each posterior femoral condyle. Total heating time was 90 s.

The modified protocol for 100 °C on the femoral component was similar to the previously described one, but trochlear groove transits were repeated 8 times, and posterior condyles required 20-s pulses. Total heating time was 200 s.

To attain 70 °C on the tibial component, PDSIH was manually held 5 mm from the surface, with the potentiometer knob fixed at 100%. It was held static over the center of the tibial plateau for 10 s. Posteriorly, two 5-s pulses were applied to each compartment, alternating sides. Total heating time was 30 s.

Modified protocol for 100 °C on the tibial component started as previously described, but an extra 10-s pulse was added to each tibial compartment. Total heating time was 50 s.

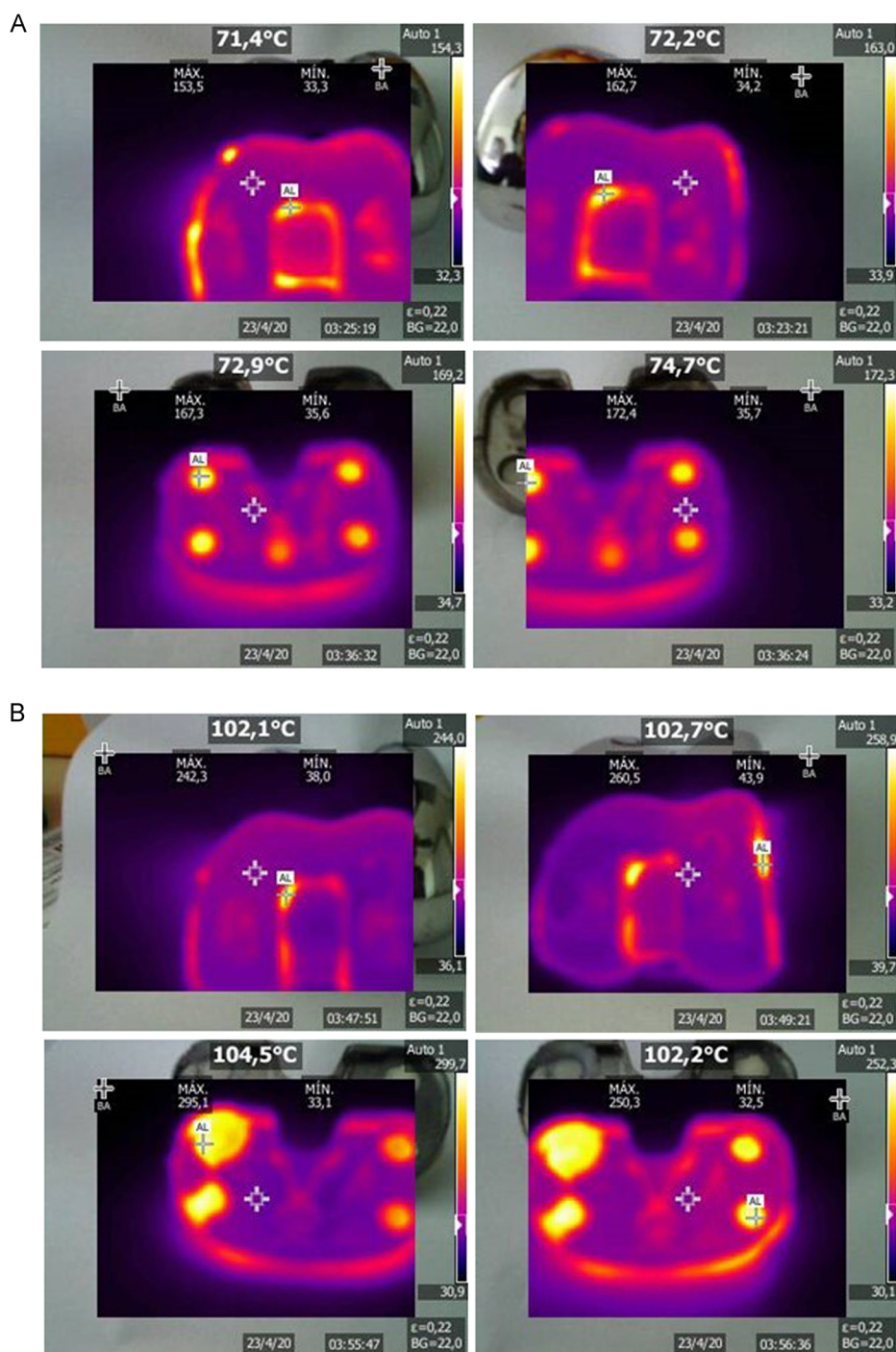
The standard 70 °C, 3.5 min protocols are schematically depicted in Fig. 2.

Surface temperature was continuously monitored with a thermographic camera (Fluke® TiS75+) with emissivity fixed as 0.22. Five-second pulses were applied on demand to each compartment to keep surface temperature stable for 210 s. Figure 3 shows characteristic thermographic images during these heating protocols.

2.4 Spectroscopic characterization

From a structural perspective, PMMA can be divided into isotactic, syndiotactic and atactic depending on the

Fig. 3 Thermographic imaging after induction heating protocols using PDSIH. **A** Protocol 1, 70 °C for 3.5 min. **B** Protocol 2, 100 °C for 3.5 min



location of lateral methyl and methyl-ester groups. The proportion of these isomers may determine the micro-structural properties and mechanical behavior of the polymer [13]. Raman spectroscopy and ATR-FTIR both register the availability of different vibrational modes in the molecules involved, and thus allow us to assess potential structural changes following induction-heating treatment.

2.5 Raman spectroscopy

As Raman spectroscopy is sensitive to both the isotactic and syndiotactic PMMA structures, this technique allowed us to assess the content of different stereoisomers in both bone cements. It was also useful for detecting other components besides PMMA polymer in bone cements, for example

radiopaque additives such as barium sulfate or zirconium dioxide [14, 15].

Sample areas from both cement products (gentamicin-loaded and antibiotic-free) were selected from the layer adjacent to the fixation surface on tibial and femoral components. In prostheses subjected to induction heating (Protocol 1, 70 °C and Protocol 2, 100 °C), sample areas were selected from regions that reached the highest temperatures according to thermographic monitoring (Fig. 3). Three-four Raman spectra were obtained for each sample area using a Raman confocal spectrometer Alpha 300 M+ (Oxford Instruments) with a 785 nm laser working at 55 mW power, with a 6 s integration time and ≥ 10 accumulations. All spectra were normalized to the intensity of the 1728 cm^{-1} band, corresponding to vibration of the C=O group. The relative intensities of the 602 cm^{-1} and the 558 cm^{-1} bands, corresponding to syndiotactic and isotactic PMMA respectively, were assessed. Also, the area ratio between the 1640 cm^{-1} and the 1728 cm^{-1} bands was calculated, which is related to the presence of methylmethacrylate monomer. The results reported hereafter correspond to tibial components, as similar results were obtained for femoral components.

2.6 Infrared spectroscopy

ATR-FTIR was selected for its sensitivity with respect to changes in the crystalline fraction of PMMA [16–18].

Cement samples of both PMMA products were selected from areas that reached the highest temperatures in femoral components. ATR-FTIR spectra were obtained with a VERTEX 70 (Bruker) spectrometer with diamond accessory, with a 4 cm^{-1} resolution in the 600–4000 cm^{-1} rank. Opus (Bruker) software was used for baseline correction and normalizing. Measurements were focused on the 882 cm^{-1} , 1295 cm^{-1} and 1339 cm^{-1} bands, which are sensitive to changes in PMMA crystallinity, and have been used to assess the evolution of the crystalline component of PMMA polymer after annealing between 90 °C and 120 °C [18–20].

3 Results

3.1 Raman spectroscopy

Raman spectroscopy allowed discrimination between antibiotic free and gentamicin loaded bone cements. In addition, it was possible to detect ZrO_2 , which is used as a radiopaque agent in the gentamicin-loaded PMMA. Some of the Raman bands of ZrO_2 , namely the bands at 554 cm^{-1} and 610 cm^{-1} , overlapped the 558 cm^{-1} and 602 cm^{-1} bands corresponding to isotactic and syndiotactic PMMA, respectively. This was not the case for the antibiotic-free

cement, as the radiopaque additive was BaSO_4 . Representative Raman spectra of PMMA with and without antibiotic (Fig. 4A), as well as a comparison between gentamicin-loaded PMMA and ZrO_2 are shown (Fig. 4B).

The intensities of the 602 cm^{-1} and the 558 cm^{-1} bands in the Raman spectra of both bone cements allowed us to estimate the relative amounts of syndiotactic and isotactic PMMA, respectively. A comparison between bone cements with and without antibiotic in the region containing the 558 cm^{-1} and 602 cm^{-1} bands, indicating also the ZrO_2 contribution, is shown in Fig. 5. In the control group, not subjected to induction heating protocols, the isotactic/syndiotactic ratios were 0.27(± 0.02) for the antibiotic-free cement, and 0.41(± 0.02) for gentamicin-loaded cement (Table 1). Therefore, both bone cements were predominantly syndiotactic, as confirmed by Raman spectroscopy.

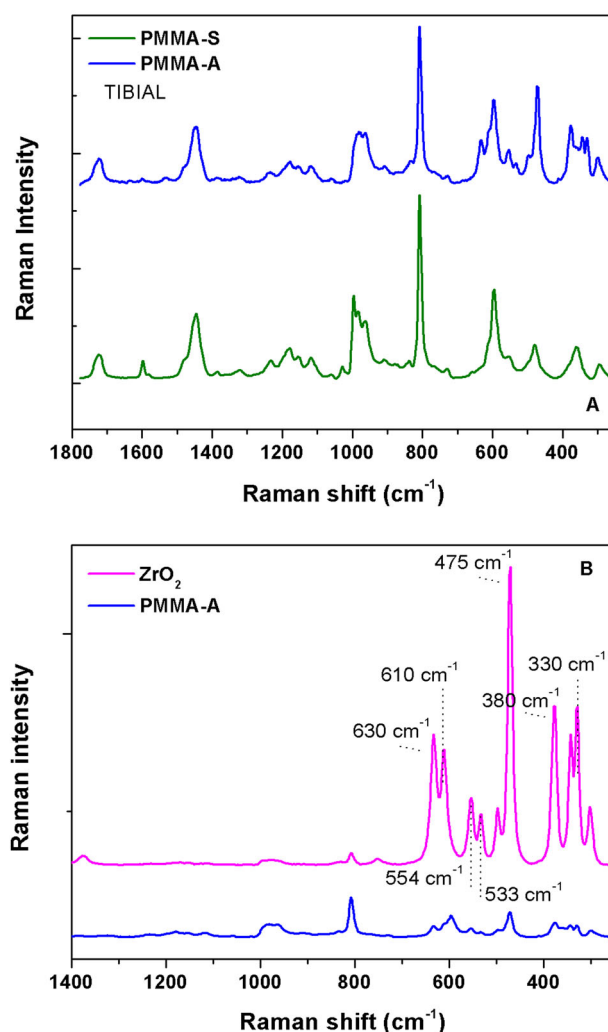


Fig. 4 **A** Representative Raman spectra of antibiotic-free (PMMA-S) and gentamicin-loaded (PMMA-A) cement. **B** Representative Raman spectra of gentamicin-loaded PMMA and ZrO_2

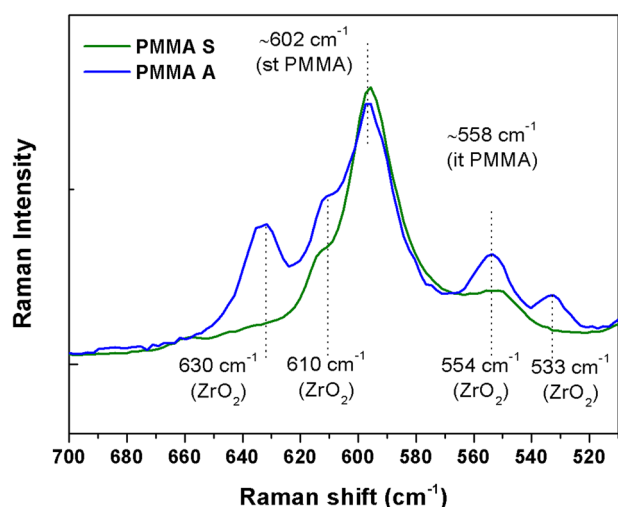


Fig. 5 Raman spectra of antibiotic-free (PMMA-S) and gentamicin-loaded (PMMA-A) cement in the 500 cm^{-1} –700 cm^{-1} region. The 558 cm^{-1} (isotactic PMMA) and 602 cm^{-1} (syndiotactic PMMA) bands, as well as the ZrO_2 contribution, are indicated

Table 1 Intensities of the 558 and 602 cm^{-1} bands (relative fraction $\pm 95\%$ CI) in control samples

	558 cm^{-1} / 1728 cm^{-1}	602 cm^{-1} / 1728 cm^{-1}	558 cm^{-1} / 602 cm^{-1}
	ISOTACTIC	SYNDIOTACTIC	I/S RATIO
Antibiotic-free PMMA	0.81 ± 0.13	2.97 ± 0.33	0.27 ± 0.02
Gentamicin-loaded PMMA	1.28 ± 0.07	3.14 ± 0.01	0.41 ± 0.02

Upon induction heating protocols, both bone cements experienced some changes in their Raman signal, specifically in the 500 cm^{-1} –700 cm^{-1} region of their Raman spectra (Fig. 6A–D). Thus, antibiotic-free cement showed increases in the relative intensity of the 558 cm^{-1} band up to $0.86(\pm 0.04)$ and $0.87(\pm 0.06)$ after the 70 °C and 100 °C protocols, respectively. However, gentamicin-loaded cement presented decreases in the 558 cm^{-1} band, down to $0.86(\pm 0.13)$ and $0.86(\pm 0.03)$ after the 70 °C and 100 °C protocols, respectively. Despite the changes observed, both bone cements kept being predominantly syndiotactic upon induction heating, as reflected in the isotactic/syndiotactic intensity ratio results (Table 2).

The presence of methylmetacrylate monomer was assessed by means of the area ratio between the 1640 cm^{-1} and the 1728 cm^{-1} bands. For antibiotic-free cement, this area ratio was $0.04(\pm 0.04)$ for the control sample, whereas it slightly decreased for samples subjected to induction heating protocols, down to $0.03(\pm 0.02)$ and $0.02(\pm 0.02)$ after Protocol 1 and Protocol 2, respectively. As for the gentamicin-loaded

cement, the area ratio was $0.05(\pm 0.01)$ in the control sample and $0.05(\pm 0.02)$ and $0.02(\pm 0.01)$ after Protocol 1 and Protocol 2, respectively. These results suggest that electromagnetic induction protocols reduced the amount of unpolymerized methylmetacrylate in both bone cements.

3.2 ATR-FTIR spectroscopy

No significant differences were found between antibiotic-free and gentamicin-loaded cement control samples through ATR-FTIR spectroscopy. In particular, no intensity peaks were observed at the 1339 cm^{-1} , 1295 cm^{-1} and 882 cm^{-1} frequencies, which are typical crystalline sensitive bands for PMMA, suggesting that the polymer was mainly amorphous in both bone cements. Figure 7 shows representative ATR-FTIR spectra of antibiotic-free and gentamicin-loaded PMMA, focusing on the 600–1800 cm^{-1} region (6B).

After both induction heating protocols, vibrational bands at the 1339 cm^{-1} , 1295 cm^{-1} and 882 cm^{-1} frequencies were still absent in the ATR-FTIR spectra of antibiotic-free bone cement (Fig. 8). The only observed variation was a slight increase in the 1540 cm^{-1} band. These findings suggest that electromagnetic induction heating protocols promoted no significant crystallization in the antibiotic-free PMMA.

In gentamicin-loaded PMMA, no changes were observed in the ATR-FTIR spectra upon the 70 °C induction heating protocol (Fig. 9). However, a very slight increase appeared in the 1340 cm^{-1} band after the 100 °C protocol, whereas no new bands appeared at 1295 cm^{-1} and 882 cm^{-1} (Fig. 9). Also, an increase in the 1540 cm^{-1} band, similar to that registered for antibiotic-free bone cement, was observed. These results suggest that the electromagnetic induction heating at 70 °C promoted no significant crystallization in the antibiotic-free PMMA.

4 Discussion

To our knowledge, all previous studies on electromagnetic induction heating [6–9, 12] focused on the in-vitro efficacy of this technique, assessing its microbicidal activity over planktonic forms or biofilms. Translation of electromagnetic induction to clinical practice would require adapting the heating protocols to the surgical environment, as well as a comprehensive study of multiple safety concerns. In this paper, one of said safety concerns is addressed. Also, a surgically-feasible induction-heating protocol over a total knee prosthesis is described for the first time.

4.1 Raman spectroscopy

Raman spectroscopy was used to assess the content of isotactic and syndiotactic stereoisomers of PMMA by

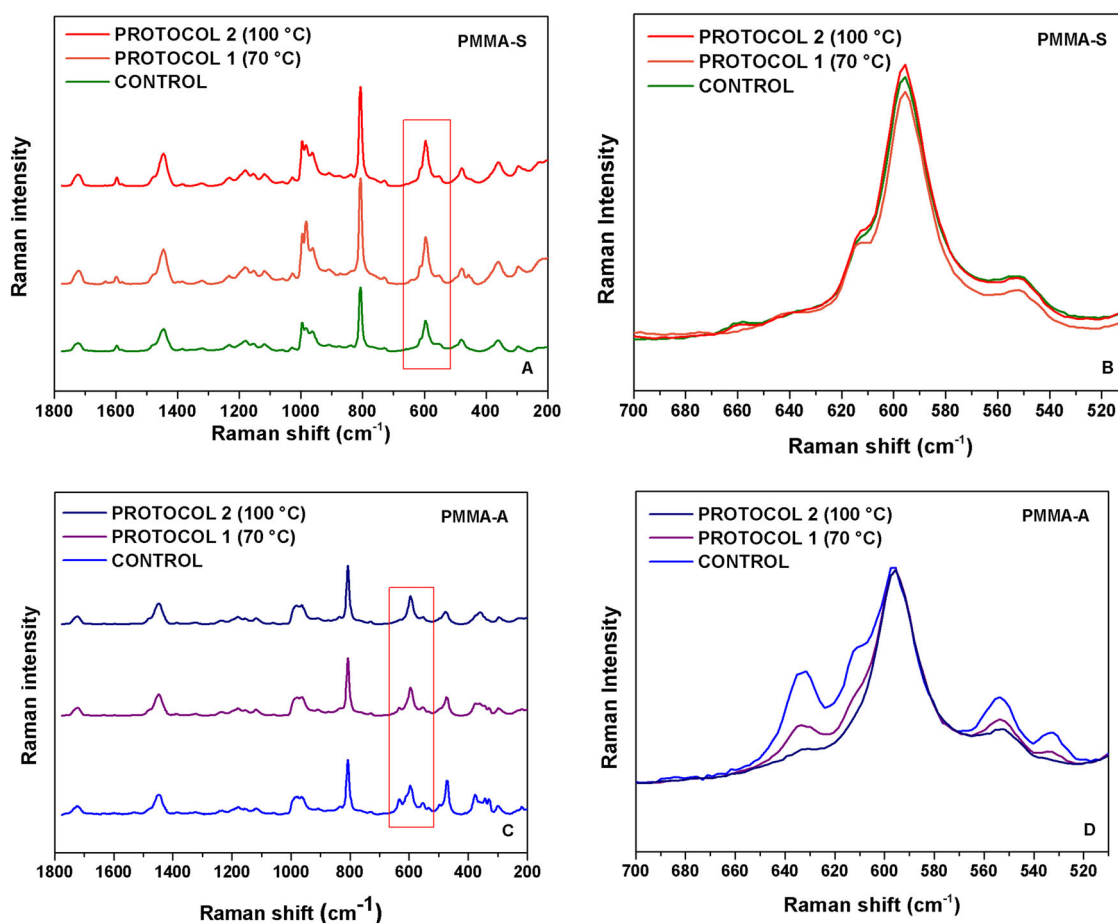


Fig. 6 Representative Raman spectra of antibiotic-free, (A) and gentamicin-loaded, (C) PMMAs subjected to induction heat protocols and zoom in of the 500 cm^{-1} –700 cm^{-1} region, (B) and (D) respectively

Table 2 Intensities of the 558 and 602 cm^{-1} bands (relative fraction $\pm 95\%$ CI) after induction heating protocols

	558 cm^{-1} / 1728 cm^{-1}	602 cm^{-1} / 1728 cm^{-1}	558 cm^{-1} / 602 cm^{-1}
ISOTACTIC		SYNDIOTACTIC	I/S RATIO
Antibiotic-free PMMA			
Control	0.81 \pm 0.13	2.97 \pm 0.33	0.27 \pm 0.02
Protocol 1 (70 °C)	0.86 \pm 0.04	2.25 \pm 0.20	0.39 \pm 0.05
Protocol 2 (100 °C)	0.87 \pm 0.06	2.38 \pm 0.12	0.36 \pm 0.02
Gentamicin-loaded PMMA			
Control	1.28 \pm 0.07	3.14 \pm 0.01	0.41 \pm 0.02
Protocol 1 (70 °C)	0.86 \pm 0.13	2.78 \pm 0.84	0.33 \pm 0.11
Protocol 2 (100 °C)	0.86 \pm 0.03	3.30 \pm 0.15	0.26 \pm 0.02

measuring the intensities of the 558 cm^{-1} and 602 cm^{-1} bands, relative to the 1728 cm^{-1} band. Both cements, antibiotic-free and gentamicin-loaded, were predominantly

syndiotactic, with isotactic/syndiotactic fractions of 0.27 and 0.41 respectively. These results may suggest that gentamicin-loaded PMMA bore a greater isotactic content. However, this difference may have been overestimated due to the contribution of a 554 cm^{-1} band representative of the ZrO_2 radiopaque additive in this cement, so this conclusion should be taken with caution.

After induction-heating, an increase in the isotactic fraction was measured in the antibiotic-free cement. On the contrary, in the gentamicin-loaded cement the isotactic content seemed to decrease down to a 0.26 fraction, similar to that of antibiotic-free PMMA. Both changes were slight and in opposite directions, but could be explained by thermal scission of lateral methoxycarbonyl groups. Although PMMA crystallization is difficult due to the high monomeric friction and the presence of methyl and methyl-ester lateral groups, these changes in the isotactic content motivated us to assess the PMMA crystallinity via ATR-FTIR spectroscopy, since this technique is sensitive to it.

Regarding the area ratio between the 1640 cm^{-1} and the 1728 cm^{-1} band, both bone cements showed very low

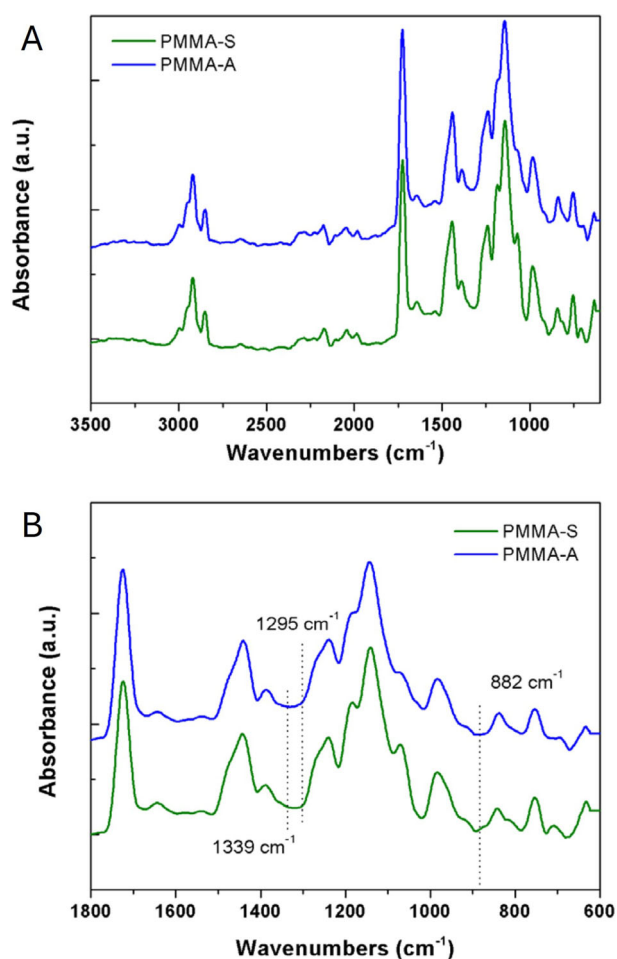


Fig. 7 **A** Representative ATR-FTIR spectra of antibiotic-free (PMMA-S) and gentamicin-loaded (PMMA-A) cement. **B** Crystalline sensitive bands, namely 1339 cm⁻¹, 1295 cm⁻¹ and 882 cm⁻¹, were absent in the 600 cm⁻¹–1800 cm⁻¹ region for both antibiotic-free (PMMA-S) and gentamicin-loaded (PMMA-A) bone cements

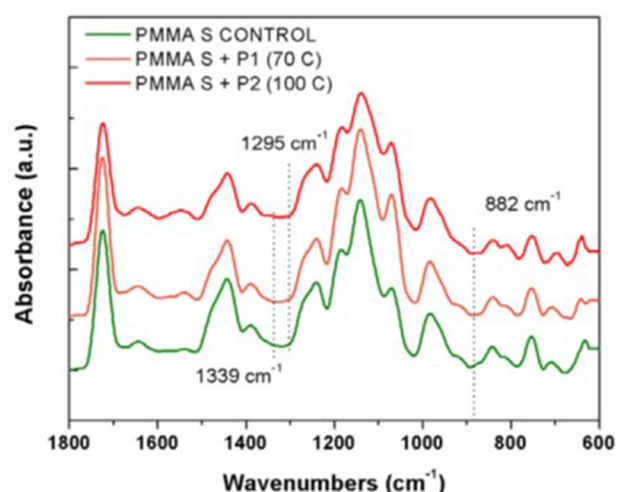


Fig. 8 ATR-FTIR spectra of antibiotic-free cement subjected to induction heating protocols. Crystalline sensitive bands, namely 1339 cm⁻¹, 1295 cm⁻¹ and 882 cm⁻¹, were absent

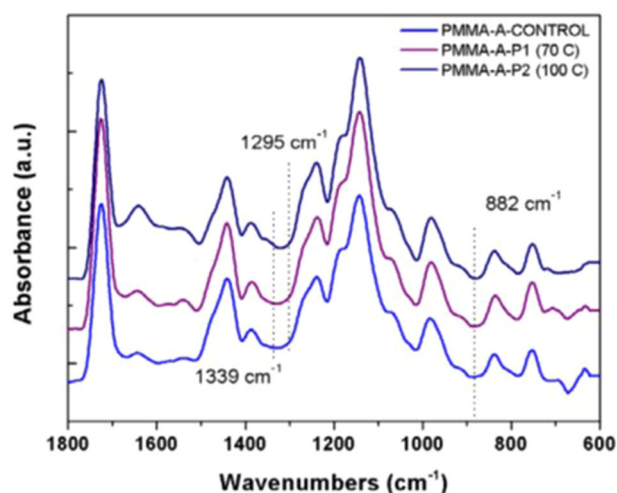


Fig. 9 ATR-FTIR spectra of gentamicin-loaded cement subjected to induction heating protocols. Crystalline sensitive bands at 1295 cm⁻¹ and 882 cm⁻¹ were absent

concentrations of methylmethacrylate monomer even in control samples. A decrease of monomer after induction heating was suggested for both cements, especially for the antibiotic-free PMMA, due to a reactivation of the polymerization process. However, these variations were very slight compared to the 95% confidence interval magnitude, and thus no conclusions can be drawn from these data.

4.2 ATR-FTIR spectroscopy

ATR-FTIR spectroscopy did not show any differences between antibiotic-free and gentamicin-loaded control samples. Variations in PMMA crystallinity after annealing processes or exposure to different solvents have been reported to show bands at 1339 cm⁻¹, 1295 cm⁻¹ and 882 cm⁻¹ [16–20]. However, no such bands were present either in control samples, or in samples subjected to the 70 °C induction heating protocol, suggesting that PMMA remained mostly amorphous even after this treatment. An isolated increase in the 1340 cm⁻¹ band was observed after the 100 °C protocol in gentamicin-loaded cement, suggesting an incipient crystallization process at this temperature.

In addition, an increase in the 1540 cm⁻¹ band was observed in both cements after induction heating protocols. This band has been previously reported to be due to an increase of C=C unsaturations after lateral methoxycarbonyl elimination [21], possibly through thermal scission.

In our view, the present findings do not imply relevant chemical or microstructural changes in the PMMA cement. These results suggest that electromagnetic induction heating disinfection techniques could be safe regarding their effects on the cement mantle.

One limitation of this study is the difficulty of Raman spectroscopy data interpretation regarding the isotactic PMMA content, due to the presence of zirconium dioxide in one of the cement products. Another limitation would be the low range of temperatures studied, because our results did not define a temperature threshold where microstructural changes begin to be relevant. However, our goal was not to define such a threshold for PMMA failure, which may be in the order of hundreds of Celsius degrees. High temperatures could imply other potential risks besides changes in the PMMA such as necrosis of adjacent host tissues, and thus are not relevant for the clinical applicability of this technique. Previous experiments in the field [6, 7, 9, 12, 22] showed that antibacterial efficacy was achieved at 70 °C, and this temperature was used to address safety to adjacent tissues in a recent study performed by our group [23], which characterized the in-vivo effect of induction heating on the adjacent bone using rabbit femora. Yet another limitation would be that only three sample groups were studied: those obtained from a standard 70 °C, 3.5-min protocol prosthesis (which would be the clinically-translatable treatment), those from a high-temperature control, and from a low temperature control, whereas other modifications of the standard protocol might also be interesting. In addition, our results may not be directly extrapolated to an in-vivo scenario, because the final temperature in the cement layer may be affected by thermal diffusion of adjacent tissues and blood supply, and the presence of fluids in a surgical environment acting as solvents may further affect the PMMA response to induction heating. Also, the absence of relevant chemical or microstructural variations does not necessarily imply that the macroscopic mechanical properties of the PMMA cement layer remain unchanged. Mechanical resistance studies, as well as in-vivo experiments assessing safety for adjacent tissues, would be needed to fully understand the safety and applicability of electromagnetic induction heating disinfection techniques. Finally, further studies regarding the quality and duration of the bone-cement interphase, along with the potential loosening of the implants in the long term, would be required.

5 Conclusions

The spectroscopic characterization performed in this study allowed us to assess potential structural changes in the PMMA bone cement after electromagnetic induction heating of orthopedic components. Variations in the isotactic and syndiotactic fractions of PMMA were observed after induction-heating protocols, probably due to lateral methoxycarbonyl thermal scission. Nevertheless, these changes were slight, and their amount and direction varied with the cement product considered. Moreover, no

changes in PMMA crystallinity were observed via ATR-FTIR spectroscopy after the standard 70 °C induction heating protocol. Only very incipient crystallization signs were noted in the safety control group subjected to a 100 °C modified protocol. Overall, our results suggest that electromagnetic induction heating generated no relevant structural changes in the PMMA cement mantle at the standard protocol conditions. Therefore, regarding its effects on the cement mantle, our standard 70 °C induction heating protocol could be regarded as a potentially feasible disinfection technique for cemented implant disinfection in total knee arthroplasty.

Data availability

The data that support the findings of this study are available from the corresponding author upon reasonable request.

Funding We disclose receipt of the following financial or material support for the research, authorship, and/or publication of this article: This study was funded within the research project FMMA2020 GOMEZ BARRENA (XVII Convocatoria de Ayudas a la Investigación, Fundación Mutua Madrileña, Spain).

Compliance with ethical standards

Conflict of interest This study was performed using a portable induction device developed by our research group, which is currently in the process of being patented. (Portable Disinfection System based on Induction Heating (PDSIH), Patent solicitude EP22382889.8). The authors have no relevant affiliations or financial involvement with any organization or entity with a financial interest in the subject discussed in the manuscript.

Publisher's note Springer Nature remains neutral with regard to jurisdictional claims in published maps and institutional affiliations.

Open Access This article is licensed under a Creative Commons Attribution-NonCommercial-NoDerivatives 4.0 International License, which permits any non-commercial use, sharing, distribution and reproduction in any medium or format, as long as you give appropriate credit to the original author(s) and the source, provide a link to the Creative Commons licence, and indicate if you modified the licensed material. You do not have permission under this licence to share adapted material derived from this article or parts of it. The images or other third party material in this article are included in the article's Creative Commons licence, unless indicated otherwise in a credit line to the material. If material is not included in the article's Creative Commons licence and your intended use is not permitted by statutory regulation or exceeds the permitted use, you will need to obtain permission directly from the copyright holder. To view a copy of this licence, visit <http://creativecommons.org/licenses/by-nc-nd/4.0/>.

References

1. McNally M, Sigmund I, Hotchen A, Sousa R. Making the diagnosis in prosthetic joint infection: a European view. *EFORT Open Rev.* 2023;8:253–63.

2. Patel R. Periprosthetic Joint Infection. *N. Engl J Med.* 2023;388:251–62. Hardin CC, editor
3. Karachalios T, Komnos GA. Management strategies for prosthetic joint infection: long-term infection control rates, overall survival rates, functional and quality of life outcomes. *EFORT Open Rev.* 2021;6:727–34.
4. Izakovicova P, Borens O, Trampuz A. Periprosthetic joint infection: current concepts and outlook. *EFORT Open Rev.* 2019;4:482–94.
5. Ciarolla AA, Lapin N, Williams D, Chopra R, Greenberg DE. Physical approaches to prevent and treat bacterial biofilm. *Antibiotics.* 2022;12:54.
6. Pijls BG, Sanders IMJG, Kuijper EJ, Nelissen RGHH. Induction heating for eradicating *Staphylococcus epidermidis* from biofilm. *Bone Jt Res.* 2020;9:192–9.
7. Pijls BG, Sanders IMJG, Kuijper EJ, Nelissen RGHH. Non-contact electromagnetic induction heating for eradicating bacteria and yeasts on biomaterials and possible relevance to orthopaedic implant infections. *Bone Jt Res.* 2017;6:323–30.
8. Pijls BG, Sanders IMJG, Kuijper EJ, Nelissen RGHH. Segmental induction heating of orthopaedic metal implants. *Bone Jt Res.* 2018;7:609–19.
9. Pijls BG, Sanders IMJG, Kuijper EJ, Nelissen RGHH. Effectiveness of mechanical cleaning, antibiotics, and induction heating on eradication of *Staphylococcus aureus* in mature biofilms. *Bone Jt Res.* 2022;11:629–38. Sep 1
10. Berman AT, Spence J, Yanicko DR, Sih GC, Zimmerman MR. Thermally induced bone necrosis in rabbits: relation to implant failure in humans. *Clin Orthop.* 1984;186:284–292.
11. Mjöberg B, Pettersson H, Rosenqvist R, Rydholm A. Bone cement, thermal injury and the radiolucent zone. *Acta Orthop Scand.* 1984;55:597–600.
12. Verheul M, Drijfhout J, Pijls B, Nibbering P. Non-contact induction heating and SAAP-148 eliminate persisters within MRSA biofilms mimicking a metal implant infection. *Eur Cell Mater.* 2021;42:34–42.
13. Greyling G, Pasch H. Tacticity separation of poly(methyl methacrylate) by multidetector thermal field-flow fractionation. *Anal Chem.* 2015;87:3011–8.
14. Taddei P, Affatato S. Comparative Raman study on the molecular structure and IN VIVO wear of poly(methyl methacrylate)-based devices used as temporary knee prostheses: Effect of the antibiotic. *J Mech Behav Biomed Mater.* 2021;116: 104328.
15. Kusaka R, Kumagai Y, Watanabe M, Sasaki T, Akiyama D, Sato N, et al. Raman identification and characterization of chemical components included in simulated nuclear fuel debris synthesized from uranium, stainless steel, and zirconium. *J Nucl Sci Technol.* 2023;60:603–13.
16. Liu J, Wang J, Li H, Shen D, Zhang J, Ozaki Y, et al. Epitaxial crystallization of isotactic poly(methyl methacrylate) on highly oriented polyethylene. *J Phys Chem B.* 2006;110: 738–42.
17. Kavda S, Golfomitsou S, Richardson E. Effects of selected solvents on PMMA after prolonged exposure: unilateral NMR and ATR-FTIR investigations. *Herit Sci.* 2023;11:63.
18. Grohens Y, Prud'homme RE, Schultz J. Cooperativity in backbone to side-chain conformational rearrangements in stereoregular PMMA. *Macromolecules.* 1998;31:2545–8.
19. Luo D, Pearce EM, Kwei TK. Miscibility of stereoregular poly(methyl methacrylates) with poly(styrene-co-p-(hexafluoro-2-hydroxy-2-propyl)styrene). *Macromolecules.* 1993;26:6220–5.
20. Dybal J, Krimm S. Normal-mode analysis of infrared and Raman spectra of crystalline isotactic poly(methyl methacrylate). *Macromolecules.* 1990;23:1301–8.
21. Holland BJ, Hay JN. The kinetics and mechanisms of the thermal degradation of poly(methyl methacrylate) studied by thermal analysis-Fourier transform infrared spectroscopy. *Polymer.* 2001;42:4825–35.
22. Enrique CGG, Medel-Plaza M, Correa JJA, Sarnago H, Acero J, Burdio JM, et al. Biofilm on total joint replacement materials can be reduced through electromagnetic induction heating using a portable device. *J Orthop Surg.* 2024;19:304.
23. Cordero García-Galán E, Medel-Plaza M, Pozo-Kreiling JJ, Sarnago H, Lucía Ó, Rico-Nieto A, et al. In vivo reduction of biofilm seeded on orthopaedic implants. *Bone Jt Res.* 2024;13:695–702.